Advanced Steel Construction – Vol. 19 No. 2 (2023) 102–111
DOI:10.18057/IJASC.2023.19.2.2

THE TENSILE PERFORMANCE OF INTER-MODULE CONNECTION WITH A BOLT AND SHEAR KEY FITTING FOR MODULAR STEEL BUILDINGS

Hong-Lei Chen [1], Cao Ke [2], Chen Chen [1] and Guo-Qiang Li [1, 3, *]

[1] *College of Civil Engineering, Tongji University, Shanghai 200092, China*
[2] *School of Management Science and Real Estate, Chongqing University, Chongqing 400044, China*
[3] *National Key Laboratory for Disaster Reduction in Civil Engineering, Tongji University, Shanghai 200001, China*
** (Corresponding author: E-mail: gqli@tongji.edu.cn)*

ABSTRACT

Modular steel buildings, as one of the most integrated prefabricated construction forms, have recently received extensive attention. The connection between modules (inter-module connection) plays a vital role in modular steel buildings' overall performance. However, most of the existing inter-module connections have problems such as insufficient construction space, difficulty in disassembly, etc. This paper proposed an innovative inter-module connection with bolt and shear key fitting, which is convenient for construction and has a clear force transmission path. The proposed connection separates the load-bearing components and has a high tolerance for installation errors. The advantages of the connection in configuration and installation were introduced, and the tensile performance of the connection was investigated with the monotonic static test. A finite element model verified with the test was also proposed to simulate the performance of the connection, and the main bearing components and failure modes of the connection were obtained through parametric study with the finite element model. Combining the experimental and numerical study results, a formula was proposed for predicting the tension capacity of the connection for practical design of inter-module connection for modular steel buildings.

ARTICLE HISTORY

Received: 30 November 2021
Revised: 26 June 2022
Accepted: 26 June 2022

KEYWORDS

Modular steel buildings;
Inter-module connection;
Bolt and shear key fitting;
Tensile performance;
Monotonic static test

1. Introduction

As one of the most integrated prefabricated steel structural forms, modular steel buildings have received widespread attention in many countries. It leads to less construction time, more cost-saving, better quality control and recycling of modules [1]. The disadvantages of modular steel buildings are that the structural span is relatively small, and the design lacks guidance and specification [2]. However, due to their special advantages, various types of modular steel buildings have been developed and used in diverse applications such as hotels, hospitals and military facilities [3].

Different from traditional steel buildings, modular steel buildings are constructed by stacking steel modules, which are manufactured off-site, transported and assembled on-site. Steel modules can be grouped into corner-supported and continuously supported, and the former is more applicable in high-rise buildings for its larger vertical bearing capacity [4]. Connections in modular steel buildings play a vital role in maintaining the strength and stability of the overall structure. As shown in Fig. 1, connections are divided into three types: inter-module, intra-module and module-foundation [2].

Considering the importance of inter-module connection in construction efficiency and load transfer, various inter-module connections have been proposed and studied [4-12]. Chen [4] proposed a new type of design with beam-to-beam connections and studied its flexural performance and aseismic behavior. Results revealed that beams and connections had independent and individual bending behaviors. Annan [5, 6] evaluated the hysteretic characteristics of modular steel building, using welding as the vertical connections and field-bolting of clip angles as horizontal connections between modules. By comparing the performance between a regular braced frame and a modular braced frame, the differences indicated that the detailing requirements of the system need to be incorporated into their design. Chen [7] investigated the seismic performance of a modular frame with pretension inter-module connection, in which the columns are vertically connected by pre-stressed strands. Chen [8] studied the tensile and shear performance of a rotary inter-module connection, and simplified calculations were developed. Lee [9] proposed a new inter-module connection to form a rigidly connected modular system and verified the seismic performance of the proposed system. Li [10, 11] proposed a splice connection and studied its performance in full-scale corner-supported modular buildings. The proposed connection was sufficient to transfer the vertical load and had a satisfactory tolerance for initial imperfections. Choi [12] adopted a bolted connection with access hole opening at the end of column in nonlinear static analyses of modular structures. It was found that the modeling of overlapped elements and the rotational behavior of connections can influence structure's lateral stiffness.

However, these connections mentioned above have some problems in the application. The most common problem is the lack of construction space, which makes it difficult to apply inter-module connections in locations with complex structures [13]. The use of welded and concrete in connections cannot give full play to the detachability of modular steel buildings. Using too many bolts in the inter-module connections will weaken the section of the members and cause the connections to be sensitive to installation errors.

In order to solve the above problems, this paper proposed an inter-module connection with a bolt and shear key fitting, which is very convenient and practical. The proposed connection separates the vertical load-bearing members from the horizontal load-bearing members. The bolts transmit the vertical loads, and the shear keys transmit the horizontal loads. The separation of load-bearing components simplifies the design and analysis of the connection. The bolt is located inside the module, not directly on the members, which allows the connection work to be completed inside the module and avoids the weakening of the members. The design of bolt holes and internal voids make the proposed connection have a high tolerance to installation errors. Therefore, the proposed connection can be used in various locations.

Studying the tensile performance of inter-module connections is very important to keep the structural integrity of modular buildings and is also beneficial to the application in high-rise modular buildings [14, 15]. In the event of members or modules being severely damaged by accidental actions, loads will be redistributed, and inter-module connections are supposed to provide an alternative load path to maintain the stability of the remaining structure. Different from the general working state, some inter-module connections may be subject to tension rather than compression. Therefore, in order to ensure that the inter-module connection can firmly tie the adjacent modules together, in addition to the shear performance, the tensile performance of the inter-module connection also needs to be studied. As shown in Fig. 1, the wind load will cause great tension in the inter-module connection at the bottom of the high-rise modular building when the structure's own weight is insufficient. If the tension exceeds the tensile capacity of the inter-module connection, the corners of the adjacent modules will break away, and the progressive collapse of the overall structure can even happen. In summary, it is very necessary to study the tensile performance of the inter-module connection.

This paper proposed an inter-module connection with bolt and shear key fitting that is convenient for construction and has a clear force transmission path. The structure, construction method and various advantages of the connection were introduced, and its tensile performance was studied through a monotonic static test. This article proposed a finite element model to simulate the performance of the connection and conducted a parametric study to obtain the main bearing components and multiple failure modes. Combining experimental data and finite element analysis results, a reasonable theoretical design formula was proposed.

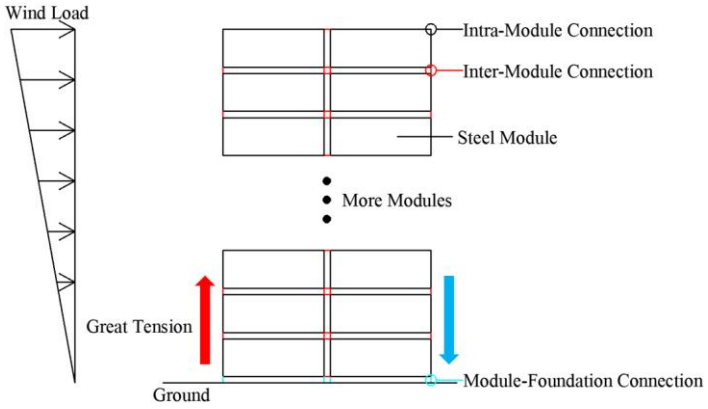

Fig. 1 Inter-module connections are under tension in some cases

2. Inter-module connection with bolt and shear key fitting

In order to facilitate design analysis and on-site installation, this paper proposed an inter-module connection with bolt and shear key fitting, in which the bolt bears most of the vertical action, and the shear key mainly bears the horizontal action [17]. Fig. 2(a) shows the construction details of the proposed connection at the corner, which is also the vertical connection of the proposed inter-module connection. The horizontal connection is achieved by sharing the same connecting plate. Its structure is simple, and the mechanism of force transmission is clear. However, the composition of vertical connection is more complex, and the internal force conditions at the vertical connection are more diverse, so this paper mainly studies the vertical connection.

The connection is composed of four parts: floor steel casting, connecting plate, ceiling steel casting and bolt. The connecting plate is located between two steel castings, and the outer contour of the connecting plate is consistent with steel casting. The shear key is welded on both sides of the connecting plate. The bolt connects two steel casting through the slotted hole on the triangular plate without contacting the connecting plate. Taking the ceiling steel casting as an example to introduce the details of the steel casting, as shown in Fig. 2(b), the ceiling steel casting consists of an L-shaped box (purple part) and a triangular plate (blue part). The L-shaped box is welded to the column and beam. The shear key hole is opened on the bottom plate (Plate P1). In addition, the two plates on the L-shaped box close to the triangular plate are called inner plates (Plate P2).

In engineering applications, after building the lower module on the flat ground, insert the shear key of the connecting plate into the ceiling steel casting's shear key hole of the lower module; then install the upper module, and the gap between the shear key and shear key hole can ensure that the shear key hole of floor steel casting is buckled with connecting plate's shear key; finally, the bolt's installation is completed in the reserved opening on the ceiling as shown in Fig. 2(a), connecting lower module's ceiling steel casting and upper module's floor steel casting.

Owing to its structure, the proposed connection has the following advantages in terms of mechanical performance and on-site construction: (1) The connection decomposes the vertical load-bearing and horizontal load-bearing components. The bolt bears most of the vertical action caused by tensile force and bending moment, while the shear key mainly bears the horizontal action caused by shear force. A clear and definite force transmission mechanism is convenient for connection analysis and design; (2) Compared with opening bolt holes at the beam end or column end, placing bolt on the triangular plate can avoid weakening members' sections and ensure the integrity of the beam and column; (3) During on-site construction, the main connection work is to install bolts after the module is positioned. The bolts are located inside the module rather than on the axis of the beam and column, overcoming the problem of insufficient construction space. Connection can be completed inside the module through the reserved opening, so the connection can be applied to various positions in the structure.

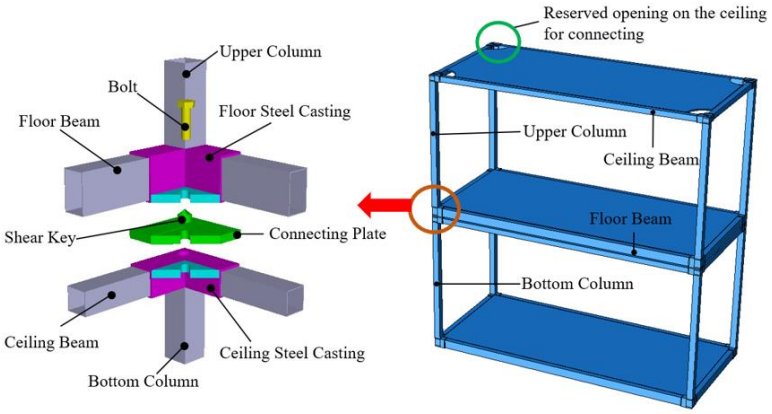

(a) Inter-module connection with bolt and shear key fitting

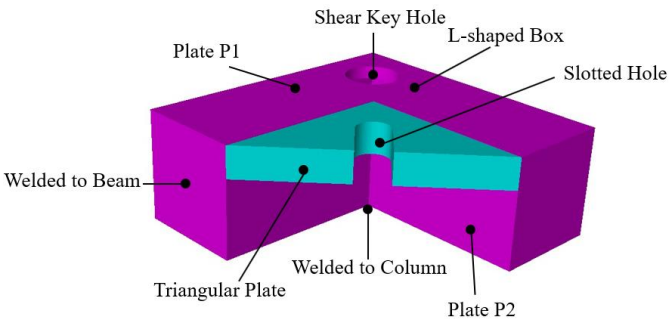

(b) Ceiling steel casting

Fig. 2 Details of the proposed connection

3. Experimental study

3.1. Materials and specimen

In the test, the 10.9-grade pressure-bearing high-strength bolts were used, and the material of members and steel casting was Q345B steel. As shown in Fig. 3, coupon tests were carried out according to the Chinese standard GB/T 228.1-2010 [16]. Three round rod specimens (Bolt1-3 and Steel1-3) were processed for the two materials. The tensile results are shown in Table 1, and the true stress-strain curve is shown in Fig. 4. Three stress-strain curves of Q345B steel basically coincide. While the curves of the bolts have certain differences, which are all within 10%.

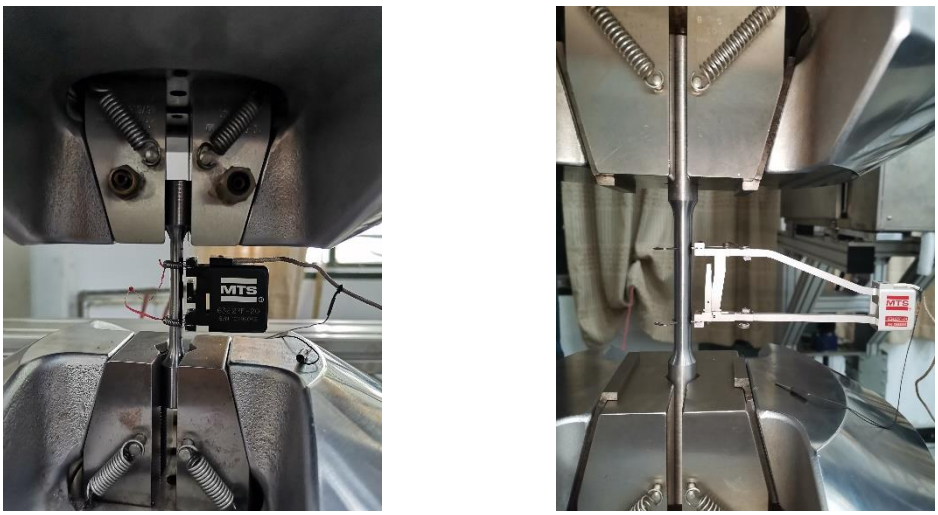

(a) Bolt specimen (b) Steel specimen

Fig. 3 Coupon tests

Table 1
Material properties

Material	Elastic Modulus (N/mm^2)	Yield Strength (N/mm^2)	Ultimate Strength (N/mm^2)	Ultimate Strain	Elongation (%)
Bolt	209766.70	1019.80	1163.67	0.04	11.30
Steel	206333.33	328.33	627.25	0.23	30.73

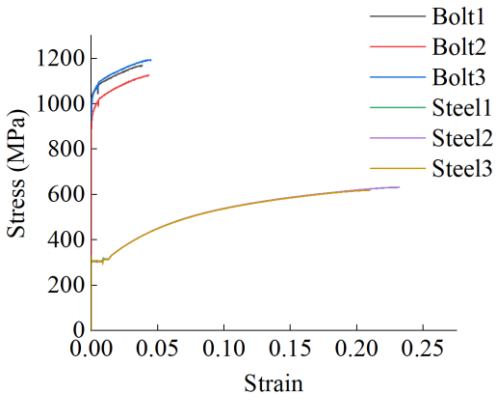

Fig. 4 Stress-strain curve of two materials

The tensile specimen in the test is shown in Fig. 5, including the top plate, upper column, connection, bottom column and bottom plate. The upper end of the upper column is welded to the top plate through stiffeners, and the lower end is welded to the connection. Similarly, the lower end of the bottom column is welded to the bottom plate through stiffeners, and the upper end is welded to the connection. The dimensions of the upper column, lower column, top plate and bottom plate are shown in Table 2. In order to facilitate production, steel castings were processed by welding.

Details of the connection's components are shown in Fig. 6. In the steel casting, the thickness of the bottom plate with the shear key hole was 25 mm (t_{bt}=25 mm), and that of the other plates was 18 mm (t_{st}=18 mm). The height of the floor steel casting was greater, and the dimensions of other parts were the same as the ceiling steel casting. In consideration of processing errors as well as facilitating construction, the diameter of the shear key hole was 4 mm larger than that of the shear key (d_{sk}=49 mm). The diameter of the bolt was 24 mm (d_b=24 mm).

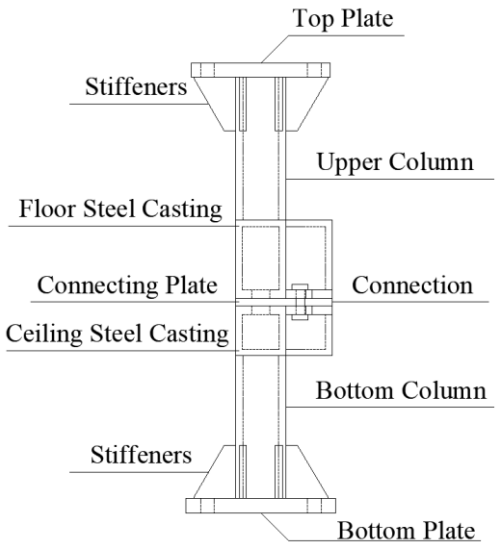

Fig. 5 Specimen

Table 2
Dimensions of the components in the tensile specimen

Member	Section Shape	Section Dimensions (mm)	Length or Thickness (mm)
Upper Column	Box	140×140×12	400
Bottom Column	Box	140×140×12	400
Top Plate	Rectangle	390×390	40
Bottom Plate	Rectangle	480×420	40

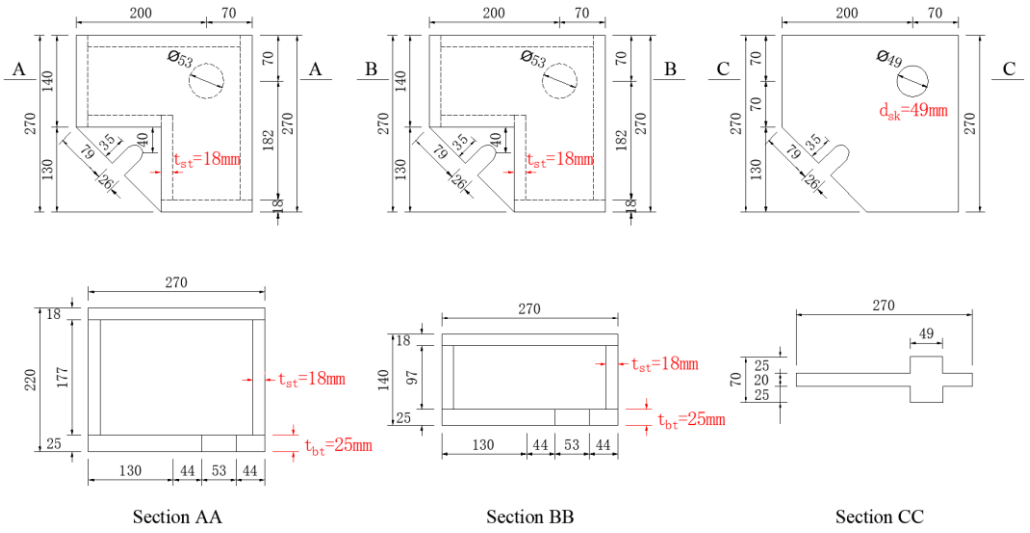

(a) Floor steel casting (b) Ceiling steel casting (c) Connecting plate

Fig. 6 Details of connection's components (unit in mm)

3.2. Experiment plan

The test setup is shown in Fig. 7. The test devices included a tensile specimen, rectangular reaction frame and 200T vertical actuator. The 200T vertical actuator was connected to the top of the specimen. The other end of the actuator is fixed on the reaction frame. The bottom plate of the specimen was connected to the reaction frame by four 36 mm-diameter bolts. The actuator applied a vertical load to the tensile specimen at a speed of 1 mm/min. And the loading will stop when the component is damaged or the load-displacement curve enters the descending section.

The measurement scheme of the experiment is shown in Fig. 8. Located at the four corners of the specimen, TD1~TD4 were vertical displacement meters used to measure the relative vertical displacement between the floor steel casting and the ceiling steel casting; TD5~TD8 were horizontal displacement meters, which were arranged symmetrically on the upper end of the floor steel casting and the lower end of the ceiling steel casting respectively to measure the horizontal displacement of the specimen. Strain gauges TS1~TS4 and TS7~TS10 were placed on the inner plate of the L-shaped box to observe the tensile strain on the inner plate; strain gauges TS5~TS6 and TS11~TS12 were placed on the triangular plate to measure the strain on the triangular plate; Strain gauge TS13 was placed on the outside of the bolt to measure the tensile strain on it.

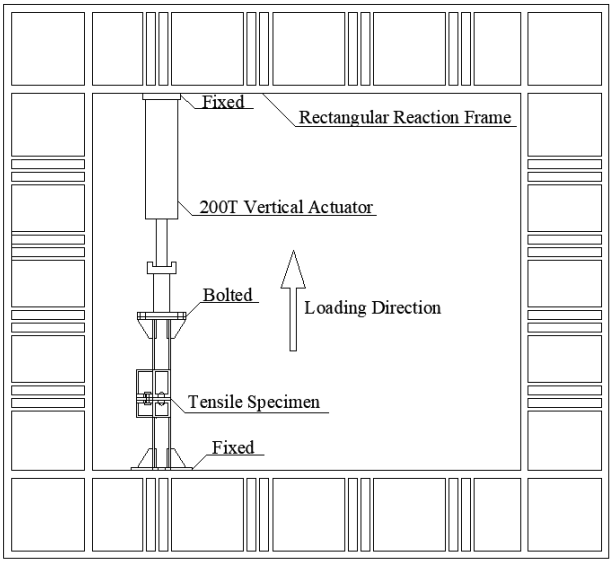

Fig. 7 Test setup

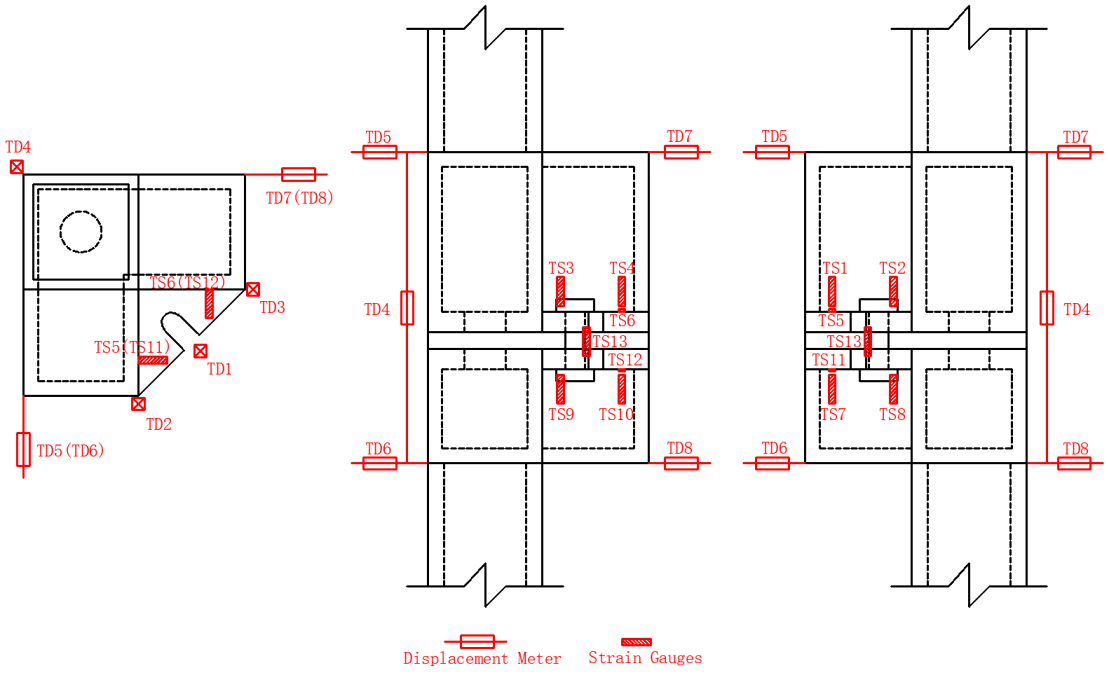

Fig. 8 Measurement scheme

3.3. Experiment results and discussion

The phenomena in the test are shown in Table 3 and Fig. 9. The failure mode of the specimen was bolt fracture, and the fracture position was in the threaded section. The load-displacement curve measured by the horizontal displacement meter TD5 and TD7 is shown in Fig. 10(a). TD5 and TD7 were located on the upper end of the floor steel casting, whose horizontal displacement was small and basically symmetrical. When the load was greater than 210 kN, the horizontal displacement at TD5 and TD7 began to increase significantly. In contrast, the horizontal displacement was very small when the load was less than 210 kN. The load-strain relationship curve measured by the strain gauge TS13 on the outside of the bolt is shown in Fig. 10(b). The tensile strain on it didn't increase monotonically. When the load was less than 103 kN, the bending deformation of the bolt was small, and the tensile strain increased. When the load was greater than 103 kN and less than 210 kN, the floor steel casting tended to rotate around the bolt. The rotation axis passed the bolt, so the tensile strain measured by TS13 decreased. When the load was greater than 210 kN, the bending deformation of the bolt was obvious, and the tensile strain of the full section of the bolt increased greatly.

Combined with the measurement results of the horizontal displacement meters TD5 and TD7 on the floor steel casting and the strain gauge TS13 on the outside of the bolt, the following conclusions can be drawn: when the load was less than 210 kN, the floor steel casting was vertically deformed; when the load was greater than 210 kN, the bolt underwent significant bending deformation, and the floor steel casting began to rotate around the bolt area. However, in actual situations, due to the overall constraint of the module, the floor steel casting cannot rotate excessively. Because the vertical displacement due to rotation is the smallest at the bolt, the relative vertical displacement of the steel castings at the bolt Δ_b is used to characterize the vertical displacement of the connection Δ_t. The Δ_b includes the deformation of the bolt and steel castings. Assuming that the steel casting rotated as a rigid body, the relative vertical displacement of the steel castings at the bolt Δ_b can be given by

$$\Delta_t = \Delta_b = td4 - \frac{td4 - td1}{l_{14}} \cdot l_{b1} \quad (1)$$

where, *tdi* is the displacement measured by displacement meter TDi, l_{b1} is the distance between the bolt and the displacement meter TD1, and l_{14} is the distance between the displacement meter TD1 and TD4.

Table 3
Phenomena in the experiment

Load (kN)	Δ_t (mm)	Phenomena	Figure
30.00	0.19	A gap of uneven width appeared between the floor steel casting and the connecting plate.	Fig 9 (a)
410.00	3.27	The floor steel casting was separated from the connecting plate; there was no obvious gap between the ceiling steel casting and the connecting plate.	Fig 9 (a)
397.60	5.54	A gap of uniform width appeared between the ceiling steel casting and the connecting plate.	Fig 9 (b)
380.60	6.28	The bolts were broken; the steel casting had no obvious cracks and deformations.	Fig 9 (c) Fig 9 (d)

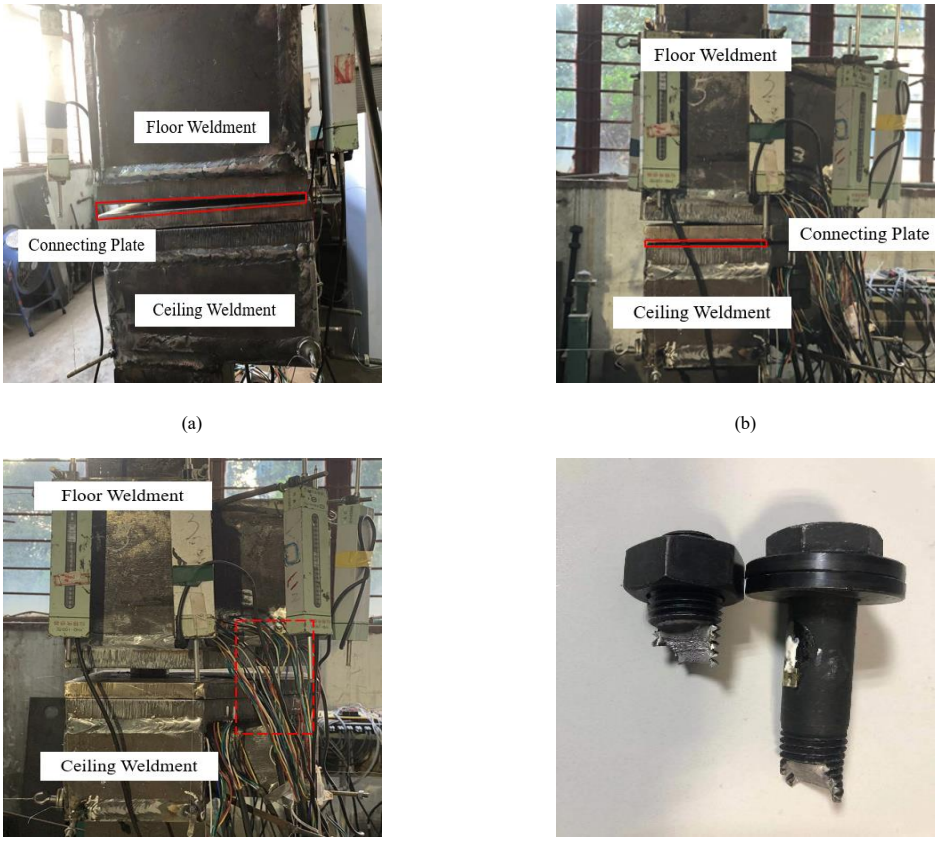

Fig. 9 Deforming state and failure behaviors in the test

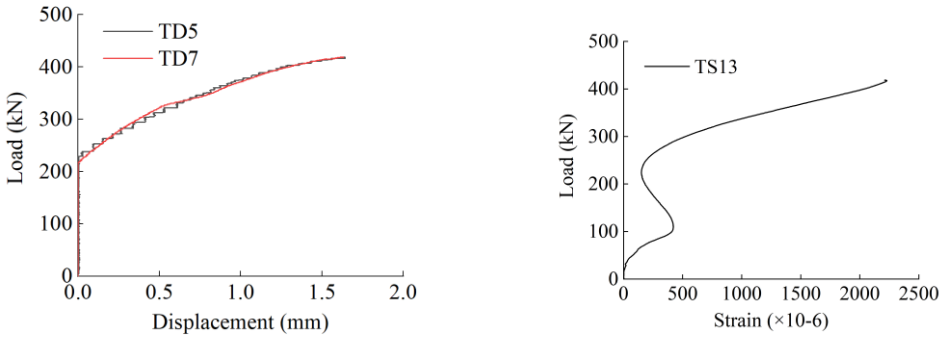

(a) Horizontal displacement (b) Tensile strain on the outside of the bolt

Fig. 10 Data curves measured by displacement meters and strain gauges

The load-displacement curve is shown in Fig. 11. The section OA of the curve is in the stage of closing the gaps, which existed inside the specimen as well as between the specimen and the reaction frame, so the tensile stiffness K_1 is relatively small. For section AB, the gaps between the components were compacted, and the stiffness remained at a relatively large value K_2. In section BC, the tensile stiffness gradually decreased until the bolt broke, reaching the ultimate bearing capacity P_{tu}=418.8 kN. For the section OA and AB, the following formula is used to calculate the equivalent initial tensile stiffness of the specimen K_{t0}=170.49 kN/mm.

$$K_{t0} = \frac{\Delta P_{OA} \cdot K_1 + \Delta P_{AB} \cdot K_2}{\Delta P_1 + \Delta P_2} \quad (2)$$

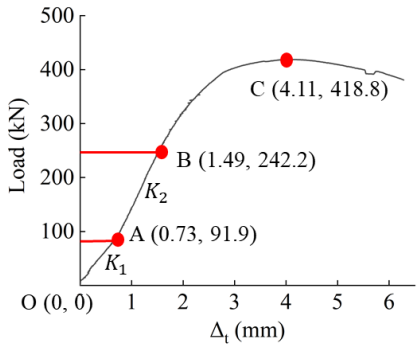

Fig. 11 Load-displacement curve of the specimen

In the test, the ultimate failure mode of the specimen was the yielding of the bolt, which was a ductile failure. This is the desired mode of failure. However, large strain values were measured on the plates of the steel casting. Therefore, in the design process, it is necessary to ensure that the steel casting is still in an elastic state when the bolt yields. In the process of data processing, considering that the connections are difficult to rotate due to the constraints inside and between the modules, the influence of the rotation of the connection under tension was minimized as much as possible. Finally, the load-displacement curve and related performance parameters of the connection under the tensile force were obtained.

4. Numerical study

4.1. Finite element model

In order to better understand the tensile performance of the bolt-shear key connection, ABAQUS was used to establish a finite element model. The dimensions and material properties of the components in the finite element model were the same as those in the experiment. In the model, the thread of the bolt was not considered. The gap between the shear key and the shear key hole, as well as the gap between the bolt and the slotted hole, was set. To ensure the accuracy of the simulation results and the normal operation of the contact, all elements of the model adopt the eight-node linear hexahedral reduction element C3D8R. The meshing result is shown in Fig. 12.

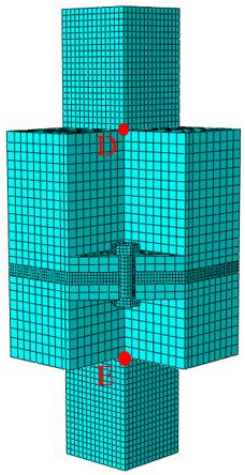

Fig. 12 Mesh of the finite element model

The members in the finite element model included the upper and bottom column, steel casting and the connecting plate. There were contacts between the steel casting and the connecting plate, between the shear key and the hole, and between the bolt and the triangular plate. The tangential behavior of contact was defined as surface contact with a friction coefficient of 0.15 [18]. And the normal behavior was defined as "hard" contact that allows separation. The relationship between columns and steel casting was simulated by tie. The fixed constraint was set at the bottom end of the bottom column, and the vertical upward displacement load was applied to the top end of the upper column.

4.2. Comparison of finite element and experiment

The load-displacement curve obtained by finite element calculation is shown in Fig. 13. Corresponding to the test, the displacement Δ_t was taken as the relative vertical displacement between the two points B and D on the steel casting near the bolt's connection area in Fig. 12. The tensile capacity and initial tensile strength obtained by the finite element analysis and experiment are shown in Table 4, and the difference between the two is relatively small. Because the bolts were broken in the threaded section and there were gaps in the experiment, the capacity and initial stiffness of the test are smaller. When the finite element model reached the ultimate capacity, the von mises stress contour plot of the connection is shown in Fig. 14. In the stress contour plot, the floor steel casting separated from the connecting plate; the bolt yielded under tension, and the stress on the inside of the bolt developed faster than the outside. The phenomenon in the finite element analysis was consistent with the experiment. According to the stress distribution of the finite element model, it can be found that the main bearing components in the tensile test are bolt, triangle plates and inner plates of steel casting.

Table 4
Comparison between experimental and numerical results

Item	Tensile Stiffness (kN/mm)	Tensile Capacity (kN)
Experimental	170.49	418.80
Numerical	185.60	436.71
Abs(error) (%)	5.93	4.28

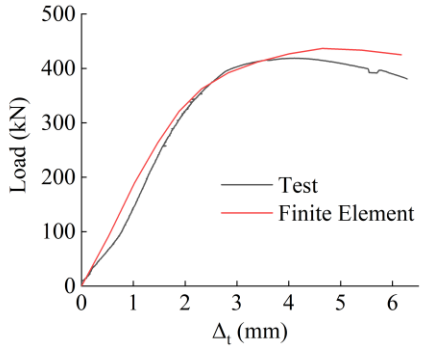

Fig. 13 Load-displacement curve of the finite element model

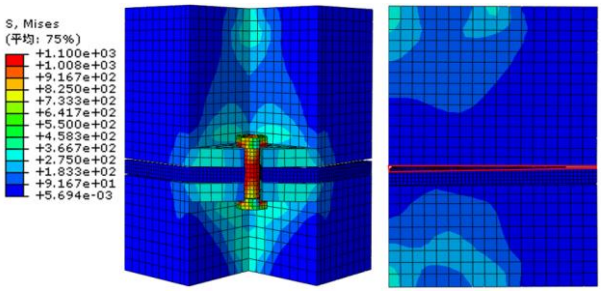

Fig. 14 Von mises stress contour plot of connection at ultimate load

4.3. Parametric study

Comparing the load-displacement curve and the experimental phenomenon, the finite element model proposed above can accurately simulate the tensile performance of the connection in the test. The proposed finite element model was used for parametric study. The parameters affecting the tensile performance of connection are: diameter of the bolt d_b, the thickness of the bottom plate of the steel casting t_{bt}, the thickness of the inner plate of the steel casting t_{st}, and diameter of the shear key d_{sk}, as shown in Fig. 6. In order to facilitate analysis and design, it is stipulated that the thickness of the other plates of the L-shaped box is the same except for the bottom plate. The thickness of the bottom plate of the L-shaped box is the same as that of the triangular plate. Through parametric study, the load-displacement curves of different dimensions' components are shown in Fig. 15, and tensile capacity's change with the dimensions of a component is shown in Fig. 16. The tensile capacity P_t is given by

$$P_t = min\left(P_{tu}, P_{t\Delta=0.02h_{cn}}\right) \tag{3}$$

where, P_{tu} is the ultimate capacity; $P_{t\Delta=0.02h_{cn}}$ is the load when displacement reached $0.02h_{cn}$; h_{cn} is the initial height of the connection.

For the parameter d_b: Shown in Fig. 15 (a), the tensile stiffness and tensile capacity of the connection increase with the increase of d_b. As shown in Fig. 16 (a), when d_b≤24 mm, the failure mode of the connection is that the bolt yields under tension; when d_b>24 mm, before the bolt yields, the steel casting has partially entered yielding, and large vertical displacement occurs. For the parameter t_{bt}: As shown in Fig. 15 (b) and Fig. 16 (b), when t_{bt}≥24 mm, the load-displacement curve changes little with the increase of t_{bt}; when t_{bt}<24 mm, the tensile stiffness of the connection is obviously reduced with the decrease of t_{bt}, and the tensile capacity is controlled by the displacement. For the parameter t_{st}: As shown in Fig. 15 (c) and Fig. 16 (c), when t_{st}≥16 mm, the tensile performance of the node does not change significantly as t_{st} increases; when t_{st}<16 mm, with the decrease of the thickness of the inner plate, the tensile capacity decreases significantly. For the parameter d_{sk}: As shown in Fig. 15 (d), the change of d_{sk} has almost no effect on the tensile performance of the connection. According to the parametric study, the main parameters that affect the tensile performance of the connection are the bolt diameter, the thickness of the bottom plate and the inner plates of the steel casting. In addition, when the bolt diameter is 24 mm, the minimum thickness of the steel casting plate is recommended to be: t_{bt}=24 mm, t_{st}=16 mm. Therefore, through parametric study, the minimum plate thickness corresponding to the bolt of a certain diameter can be obtained.

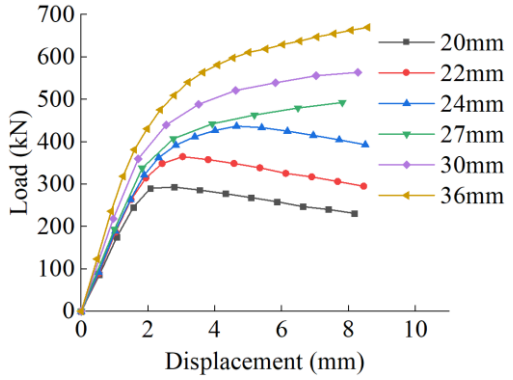

(a) diameter of bolt d_b

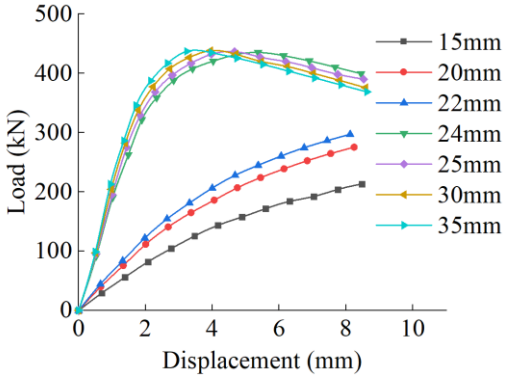

(b) thickness of the bottom plate t_{bt}

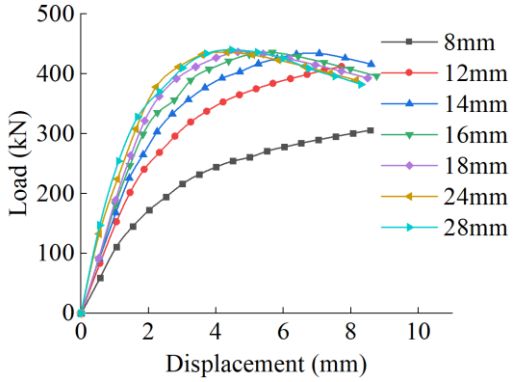

(c) thickness of the inner plate t_{st}

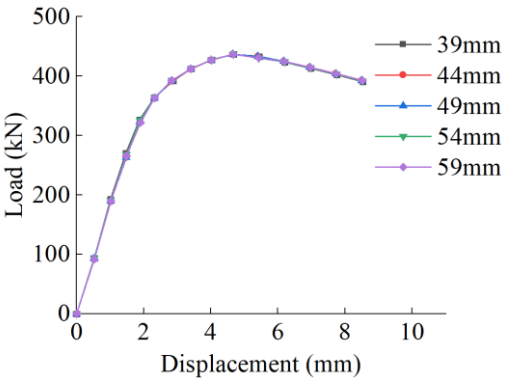

(d) diameter of the shear key d_{sk}

Fig. 15 Load-displacement curve of component's different dimensions

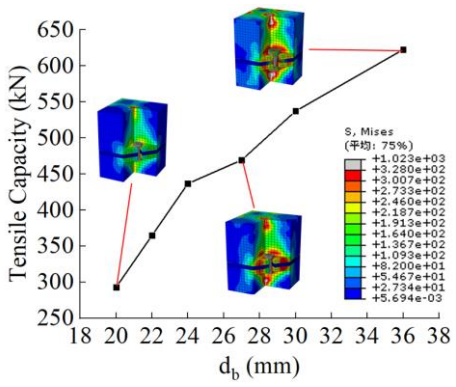

(a) diameter of bolt d_b

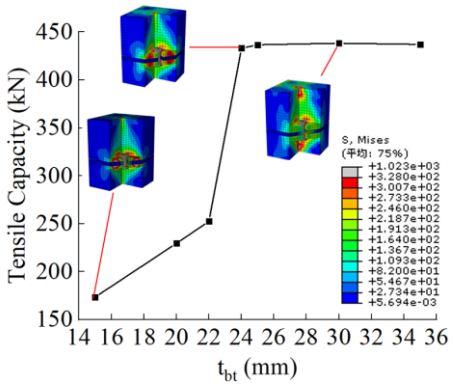

(b) thickness of the bottom plate t_{bt}

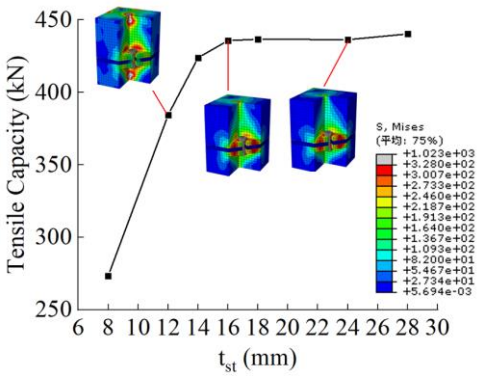

(c) thickness of the inner plate t_{st}

Fig. 16 Tensile capacity's change with the dimensions of the component

In this part, a finite element model that can well simulate the test well was proposed, whose effectiveness was verified by comparison with the experiment. Using the verified finite element model for parameter learning, it is further clarified that the main bearing components of the connection during tension are the bolt, the inner plates and the bottom plates of the steel casting. The shear key has almost no contribution to the vertical force transmission of the connection. Based on the bolt of a certain diameter determined by the vertical load between the modules, the recommended value of the minimum thickness of the steel casting plate can be obtained by parametric study.

5. Theoretical study

5.1. Theoretical analysis

According to the experimental research and finite element analysis, the parameters and components that mainly affect the tensile performance of the connection were obtained. Aiming at the failure mode of each bearing member, theoretical design formulas of tensile capacity related to the parameters were given below.

5.1.1. Failure mode 1: The bolt yields under tension

The bolt is not located on the axis of the column, so the bolt is subjected to the combined action of tensile force and bending moment, and the inner tensile strain develops faster. To be conservative, assume that the connection fails when the inner side of the bolt yields. The calculation formula of the tensile capacity P_{t1} is given by

$$P_{t1} = f_{yb}\left(\frac{1}{A_b} + \frac{l_{pb}}{W_b}\right)^{-1} \tag{4}$$

where, f_{yb} is the yield strength of the bolt; A_b is the cross-sectional area of the bolt; W_b is the flexural section coefficient of the bolt; and l_{pb} is the distance from the point of force to the bolt.

5.1.2. Failure mode 2: The L-shaped box yields under tension

As shown in Fig. 17, assuming that when the L-shaped box transmits tension, only the inner plate (red area) bears the force. Under the action of tensile force, it is assumed that the connection fails when the edge of the inner plate's section (blue line area) yields. According to the symmetry relationship, the formula for calculating the tensile capacity P_{t2} is given by

$$P_{t2} = f_{ys}\left(\frac{1}{A_{ip}} + \frac{l_{pc}}{W_{ip}}\right)^{-1} \tag{5}$$

where, f_{ys} is the yield strength of the steel casting; A_{ip} is the cross-sectional area of the inner plate; W_{ip} is the flexural section coefficient of the inner plate; and l_{pc} is the distance from the point of force to the centroid of the inner plate.

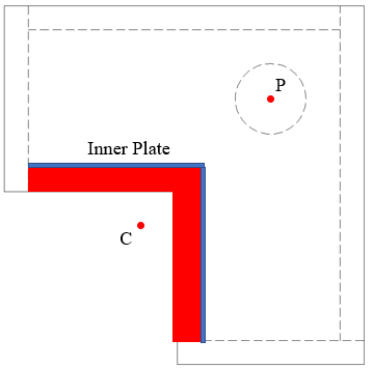

Fig. 17 The edge of the inner plate section yields

5.1.3. Failure mode 3: The triangular plate yields under tension

As shown in Fig. 18, according to the yield line theory and the stress distribution of the finite element model, there are three types of yield lines formed on the triangle plate under tension: line 1 and 3 are negative yield lines; line 2 are positive yield lines. According to the principle of virtual work, the calculation formula of internal virtual work W_{pl} is given by

$$W_1 = W_3 = m_p\left(l_{1x}\varphi_{1x} + l_{1y}\varphi_{1y}\right) = \frac{f_{ys}t_{bt}^2}{4}\frac{\sqrt{2}l_{st}}{2}\delta\frac{2\sqrt{2}}{l_{bt}} = \frac{\delta f_{ys}t_{bt}^2}{2} \tag{6}$$

$$W_2 = m_p l_2 \varphi_2 = \frac{f_{ys} t_{bt}^2}{4} l_2 \frac{2\sqrt{2}\delta}{l_{bt}} \tag{7}$$

$$W_{pl} = \sum W_i = \delta f_{ys} t_{bt}^2 \left(1 + \frac{d_d}{l_{bt}} - \frac{\sqrt{2} d_b}{4 l_{bt}}\right) \tag{8}$$

where, W_i is the virtual work done by the ith yield line; m_p is the yielding moment per unit length of the triangular plate; l_i is the length of the ith yield line; φ_i is the angle of the ith yield line; t_{bt} is the thickness of the triangular plate; l_{bt} is the side length of the triangular plate; d_d is the end distance from the bolt to the L-shaped box.

The external virtual work of the force is given by

$$W_b = P \frac{2 d_d \delta}{l_{bt}} \tag{9}$$

According to the equality of internal virtual work and external virtual work, the tensile capacity of the connection P_{t3} is given by

$$P_{t3} = \frac{f_{ys} t_{bt}^2}{2 d_d} \left(l_{bt} + d_d - \frac{\sqrt{2} d_b}{4}\right) \tag{10}$$

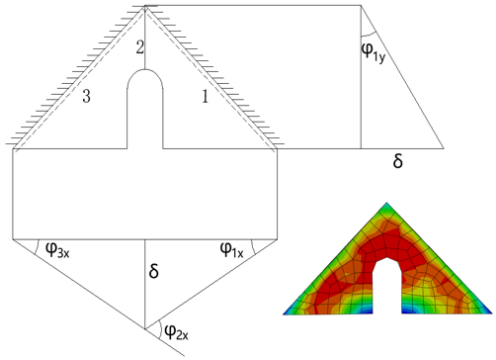

Fig. 18 Yield line distribution of triangular plate

By summarizing the above three failure modes, the tensile capacity of the connection P_t is given by

$$P_t = min(P_{t1}, P_{t2}, P_{t3})$$

$$= min\left(f_{yb}\left(\frac{1}{A_b} + \frac{l_{pb}}{W_b}\right)^{-1}, f_{ys}\left(\frac{1}{A_{ip}} + \frac{l_{pc}}{W_{ip}}\right)^{-1}, \frac{f_{ys} t_{st}^2}{2 d_d}\left(l_{st} + d_d - \frac{\sqrt{2} d_b}{4}\right)\right) \tag{11}$$

5.2. Comparison of the theoretical analysis against experimental results and parametric study

In engineering applications, we suggest that the failure mode of the connection under tensile force is the bolt yielding, which is convenient for the replacement and monitoring of the bolt. Therefore, the tensile capacity corresponding to other failure modes should be greater than that corresponding to the bolt yielding. After formula (4) is used to determine the bolt's diameter according to the tension requirements of the connection, the minimum thickness of the inner plates and bottom plate of the steel casting can be obtained by the above formula (5, 10). Assuming that the bolt diameter d_b=24 mm, the tensile capacity of the connection and the thickness of the steel casting can be calculated by the theoretical design formula. As shown in Table 5, the tensile capacity of the connection obtained by the numerical and theoretical analysis is basically consistent. Since the bolt broke in the threaded section in the experiment, the tensile capacity is relatively small. The comparison of the minimum thickness of the steel casting between the theoretical and numerical study is shown in Table 6. The minimum thickness of the steel casting calculated by the theoretical design formula is greater than that of the parametric study, and the difference between the two is not large. Results indicated that the theoretical calculation formula could reasonably design the bolt's diameter and the minimum thickness of the steel casting.

Table 5
Comparison of tensile capacity

Item	P_t (kN)	Abs(error) (%)
Experimental	418.80	
Numerical	436.71	4.28
Theoretical	434.44	3.73

Table 6
Comparison of the minimum thickness of plates between theoretical formula and parametric study

Item	P_t (kN)	t_{bt} (mm)	t_{st} (mm)
Numerical	436.71	24	16
Theoretical	434.44	26	18
Abs(error) (%)	0.52	8.33	12.50

Compared to complex parametric learning, more practical theoretical design formulas were proposed based on the conclusions of the experiment and finite element analysis. Through the theoretical design formula, the bolt diameter that can safely transmit the tension between the modules can be obtained, as well as the minimum thickness of the steel casting' plates corresponding to the bolt's diameter. The comparison with the parameter learning's results proved the practicability and rationality of the theoretical design formulas.

6. Conclusions

In order to reliably and conveniently connect modules of modular steel structure buildings, a novel bolt and shear key fitting was proposed for the inter-module connection, which has the advantages of easy installation, clear force transmission path and high tolerance to installation errors. This paper conducted both experimental and numerical studies on the tensile performance of the connection, and formula was proposed for predicting the tensile capacity of the connection. The following conclusions can be summarized:

(1) To facilitate design and analysis, the proposed inter-module connection decomposes the vertical load-bearing and horizontal load-bearing components, in which the bolt bears most of the vertical action, and the shear key mainly bears the horizontal action. The bolts are located inside the module, and on-site installation can be completed inside the module through the reserved opening. The slotted hole, as well as the gap between shear key and shear key hole, can provide high tolerance to installation errors.

(2) In the tensile test, the main bearing components included the bolt, the triangle plate and the inner plates of the steel casting, on which significant strain has been monitored. The ultimate failure mode of the specimen was the tensile yielding of the bolt. It is the expected failure mode because the bolt is easy to replace.

(3) By comparing the measured data and experimental phenomena, it is proved that the finite element model proposed can simulate the tensile performance of the connection in the test. Observing the stress distribution of the finite element model, it can be found that the main bearing component of the L-shaped box is the inner plate.

(4) Through parametric study, it is found that the tensile failure modes of the connection include bolt yielding, triangular plate yielding, and inner plate yielding. The size of the shear key has nothing to do with the tensile performance of the connection. According to the results of the parametric study, when the bolt's diameter is 24 mm, the recommended value of the inner plates' minimum thickness is 16 mm, and the recommended value of the bottom plate's minimum thickness is 24 mm.

(5) Combining experimental phenomena and numerical analysis, the theoretical design formula of the tensile capacity of the connection was obtained. According to the calculation of the theoretical design formula, when the bolt diameter is 24 mm, the minimum thickness of the inner plate of the steel casting is 18 mm, and the minimum thickness of the bottom plate is 26 mm, which is slightly larger than the result obtained by the parametric study. And the tensile capacity of the experiment is not much different from numerical and theoretical analysis. The theoretical formula can reasonably design the proposed inter-module connection.

Acknowledgements

The research work presented hereinabove was supported by the National Key Research and Development Program of China (Project No.2017YFC0703803-04) and the National Science Foundation for Young

Scientists of China (Grant No.51808068).

References

[1] F.J. Luo, C. Ding, A. Styles, Y. Bai, End Plate-Stiffener Connection for SHS Column and RHS Beam in Steel-Framed Building Modules, International Journal of Steel Structures, 19 (2019) 1353-1365.
[2] A.W. Lacey, W.S. Chen, H. Hao, K.M. Bi, Structural response of modular buildings - An overview, Journal of Building Engineering, 16 (2018) 45-56.
[3] R. Sanches, O. Mercan, B. Roberts, Experimental investigations of vertical post-tensioned connection for modular steel structures, Engineering Structures, 175 (2018) 776-789.
[4] Z.H. Chen, J.D. Liu, Y.J. Yu, Experimental study on interior connections in modular steel buildings, Engineering Structures, 147 (2017) 625-638.
[5] C.D. Annan, M.A. Youssef, M.H. El Naggar, Experimental evaluation of the seismic performance of modular steel-braced frames, Engineering Structures, 31 (2009) 1435-1446.
[6] C.D. Annan, M.A. Youssef, M.H. El Naggar, Seismic Overstrength in Braced Frames of Modular Steel Buildings, Journal of Earthquake Engineering, 13 (2009) 1-21.
[7] Z. Chen, H. Li, A. Chen, Y. Yu, H. Wang, Research on pretensioned modular frame test and simulations, Engineering Structures, 151 (2017) 774-787.
[8] Z.H. Chen, J. Wang, J.D. Liu, Z.Y. Cong, Tensile and shear performance of rotary inter-module connection for modular steel buildings, Journal of Constructional Steel Research, 175 (2020) 15.
[9] S. Lee, J. Park, E. Kwak, S. Shon, C. Kang, H. Choi, Verification of the Seismic Performance of a Rigidly Connected Modular System Depending on the Shape and Size of the Ceiling Bracket, Materials, 10 (2017).
[10] G.-Q. Li, K. Cao, Y. Lu, Column effective lengths in sway-permitted modular steel-frame buildings, Proceedings of the Institution of Civil Engineers-Structures and Buildings, 172 (2019) 30-41.
[11] Y.-F. Lyu, G.-Q. Li, K. Cao, S.-Y. Zhai, H. Li, C. Chen, Y.-Z. Wang, Behavior of splice connection during transfer of vertical load in full-scale corner-supported modular building, Engineering Structures, 230 (2021).
[12] Kyung-Suk Choi, Ho-Chan Lee, Hyung-Joon Kim, Influence of Analytical Models on the Seismic Response of Modular Structures, Journal of The Korea Institute for Structural Maintenance and Inspection, 20 (2016) 74-85.
[13] X.-M. Dai, L. Zong, Y. Ding, Z.-X. Li, Experimental study on seismic behavior of a novel plug-in self-lock joint for modular steel construction, Engineering Structures, 181 (2019) 143-164.
[14] P.M. Lawson, M.P. Byfield, S.O. Popo-Ola, P.J. Grubb, Robustness of light steel frames and modular construction, Structures & Buildings, 161 (2008) 3-16.
[15] R.M. Lawson, J. Richards, Modular design for high-rise buildings, Proceedings of the Institution of Civil Engineers-Structures and Buildings, 163 (2010) 151-164.
[16] GB/T 228.1-2010. Metallic materials-Tensile testing-Part 1: Method of test at room temperature, in, Standards Press of China, Beijing, 2010. (in Chinese)
[17] Guo-Qiang Li, Hong-Lei Chen,Chen Chen, Cast steel connections between modules. China Patent: ZL201810883013.6,December 4, 2020. (in Chinese)
[18] Tian-Hong Zheng, Theoretical and experimental study on friction model, in, Guizhou University, (2020) 59-61.